Cancer Cell
Article

Virus-Tumor Interactome Screen Reveals ER Stress Response Can Reprogram Resistant Cancers for Oncolytic Virus-Triggered Caspase-2 Cell Death

Douglas J. Mahoney,[1,2] Charles Lefebvre,[1,2] Kristina Allan,[1] Jan Brun,[1,2] Cina A. Sanaei,[1] Stephen Baird,[1,2] Nelson Pearce,[1] Susanna Grönberg,[1] Brian Wilson,[5] Mikael Prakesh,[5] Ahmed Aman,[5] Methvin Isaac,[5] Ahmed Mamai,[5] David Uehling,[5] Rima Al-Awar,[5] Theresa Falls,[4] Tommy Alain,[6] and David F. Stojdl[1,2,3,*]

[1]Children's Hospital of Eastern Ontario Research Institute, Ottawa, Ontario K1H 8L1, Canada
[2]Department of Pediatrics
[3]Department of Biochemistry, Microbiology, and Immunology
University of Ottawa, Ottawa, Ontario K1H 8L1, Canada
[4]Ottawa Hospital Research Institute, Center for Cancer Therapeutics, 501 Smyth Road, 3rd Floor, Box 926, Ottawa, Ontario K1H 8L6, Canada
[5]Medicinal Chemistry Platform, Ontario Institute for Cancer Research, MaRS Center, 101 College Street, Toronto, Ontario M5G 0A3, Canada
[6]Department of Biochemistry and Goodman Cancer Research Centre, McGill University, Montreal, Quebec H3A 1A3, Canada
*Correspondence: dave@arc.cheo.ca
DOI 10.1016/j.ccr.2011.09.005

SUMMARY

To identify therapeutic opportunities for oncolytic viral therapy, we conducted genome-wide RNAi screens to search for host factors that modulate rhabdoviral oncolysis. Our screens uncovered the endoplasmic reticulum (ER) stress response pathways as important modulators of rhabdovirus-mediated cytotoxicity. Further investigation revealed an unconventional mechanism whereby ER stress response inhibition preconditioned cancer cells, which sensitized them to caspase-2-dependent apoptosis induced by a subsequent rhabdovirus infection. Importantly, this mechanism was tumor cell specific, selectively increasing potency of the oncolytic virus by up to 10,000-fold. In vivo studies using a small molecule inhibitor of IRE1α showed dramatically improved oncolytic efficacy in resistant tumor models. Our study demonstrates proof of concept for using functional genomics to improve biotherapeutic agents for cancer.

INTRODUCTION

Despite major advances in our understanding of cancer over the last 50 years, it remains one of the most important health challenges worldwide. Innovative approaches are needed to complement current therapeutic strategies, and oncolytic viruses represent one such promising tool in the fight against cancer (Vähä-Koskela et al., 2007). In oncolytic virus therapy (OVT), replicating viruses selectively target tumors based on the genetic abnormalities of their malignant cells, including aberrant cell division, innate immune defects, and tumor-specific gene expression (Sinkovics and Horvath, 2008). In addition to inducing direct tumor cell lysis, a productive virus infection leads to recruitment of the patient's immune system to attack the tumor (Parato et al., 2009), and modulation of the tumor vasculature to starve and kill cancer cells en masse (Breitbach et al., 2007). In aggregate, the high tumor selectivity, multimodal mechanisms for tumor destruction, and lack of genotoxicity with OVT offer great potential for increasing efficacy while eliminating the side and late effects that plague current therapeutic strategies. Over the past decade a growing number of natural and genetically modified viruses have been shown to cure disease in a diverse set of rodent tumor models (Sinkovics and Horvath, 2008; Vähä-Koskela et al., 2007). Importantly, three such virus platforms are now entering late-phase clinical trials following impressive Phase II data (Kaufman and Bines,

Significance

Although therapeutic approaches using tumor-killing viruses (oncolytic viruses) are showing great promise in human trials, with response rates in Phase II trials ranging from 30% to 70%, clearly not all patients are benefiting. In this study we screened the human genome looking for potent opportunities to sensitize cancer cells to oncolytic virus therapy. Our work reveals that tumor cells can be tricked into turning on a dormant suicide pathway by causing a mild stress to their protein-folding machinery. These "reprogrammed" tumor cells are triggered to die only when they are subsequently infected by an oncolytic virus. This "one-two punch" is cancer selective, can be induced genetically or chemically, and regresses tumors that are resistant to either therapy alone.

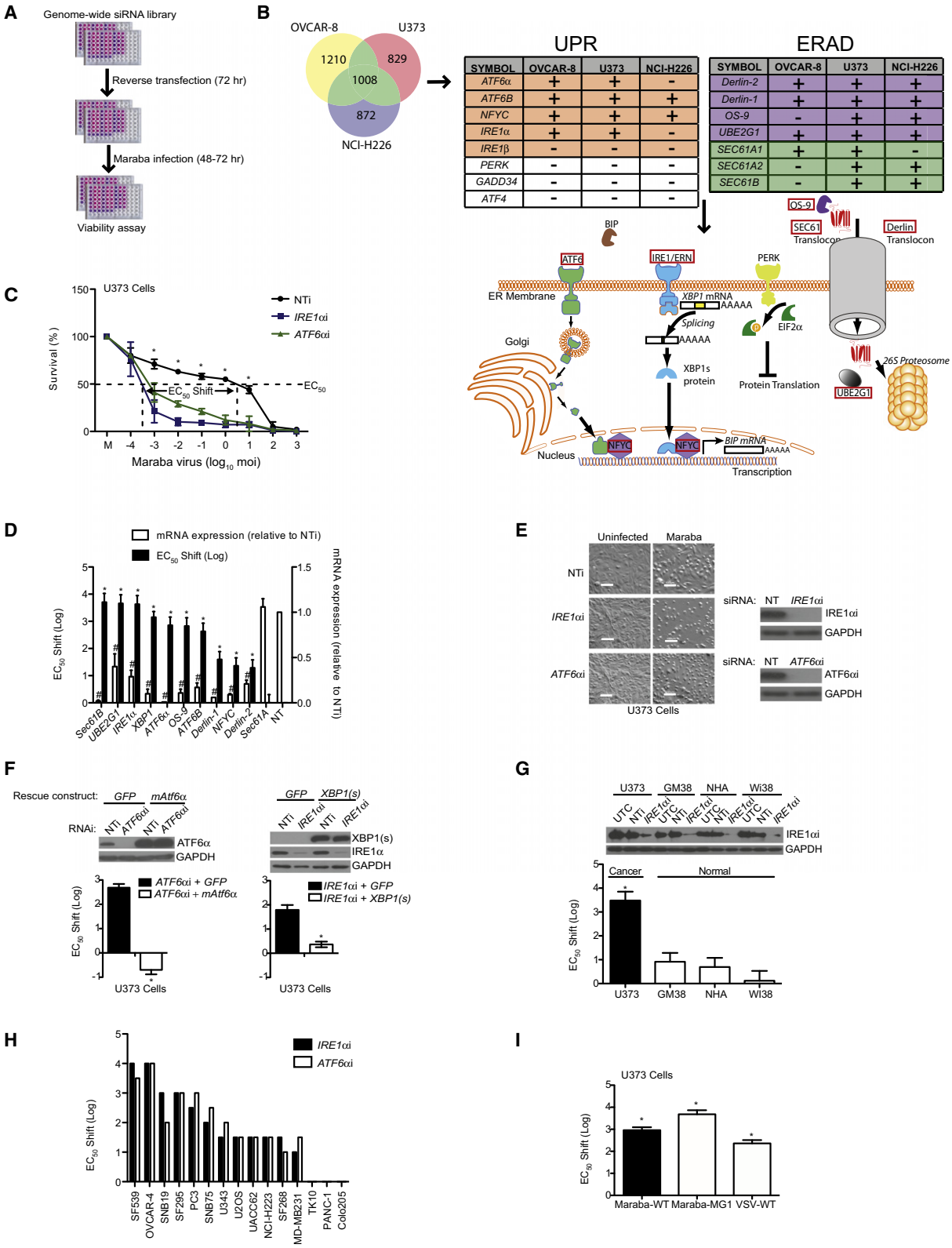

Figure 1. Genome-wide Screen Identifies ER Stress Response Blockade as a Potent Sensitizer to Rhabdovirus-Mediated Oncolysis

(A) Schematic representation of the screen.

(B) Venn diagram outlining the number of overlapping hits, and a table (+, synthetic lethal; −, no interaction) and schematic diagram (hits outlined in red) illustrating key hits within the UPR and ERAD pathways.

2010; Lal et al., 2009; D.K. Jennerex Biotherapeutics, personal communication).

Host/virus interactions at the cellular and organismal level govern the outcome of any virus encounter, including OVT. Thus far, most efforts to improve OVT have focused on genetically modifying the virus. However, the outcome of any host/virus interaction is governed by contributions from both genomes. We sought to understand the host's contribution to the oncolytic virus effect by using functional genomic screening to elucidate the molecular mechanisms that control a productive rhabdoviral infection and contribute to rhabdovirus-mediated tumor cell killing. By understanding these mechanisms in detail, we envisioned that we could engineer maximally effective therapeutic viruses, and/or design potent drug/virus combinations that exploit unforeseen biological interfaces between oncolytic viruses, the host and cancer.

RESULTS

Blockade of the Endoplasmic Reticulum (ER) Stress Response Sensitizes Cancer Cells toward Viral Oncolysis

Wild-type and engineered strains of rhabdoviruses, such as vesicular stomatitis virus (VSV) and more recently Maraba virus, have been shown to be potent oncolytic agents in several rodent models of cancer (Stojdl et al., 2000b, 2003; Balachandran and Barber, 2000; Brun et al., 2010). To search for host factors that modulate rhabdovirus-mediated oncolysis, we performed a synthetic lethal RNAi screen of the human genome across three tumor-derived cell lines (Figure 1A). We used an arrayed library of siRNA pools to target ~18,200 genes in OVCAR-8 (ovarian carcinoma), U373 (glioblastoma), or NCI-H226 (nonsmall cell lung carcinoma) cells. Transfected cells were either mock infected or infected with wild-type Maraba virus as a representative oncolytic rhabdovirus. Following infection we incubated the cells for 48–72 hr, after which we scored cell viability using resazurin vital dye. To identify primary "hits," we analyzed data from two independent screens for each cell line using the median absolute deviation method (Chung et al., 2008). Subtracting those genes scoring positively in the siRNA alone screens defined 1008 synthetic lethal hits common to at least 2 out of 3 cancer lines from the primary screen (Figure 1B, and see Table S1 available online). Subsequent bioinformatics analysis revealed an enrichment of hits within the ER stress response pathways (Figure 1B and Table S2), including members of two of the three known signaling cascades that comprise the unfolded protein response (UPR). Key hits therein included the transcription factors ATF6α and ATF6B, the endoribonucleases/protein kinase IRE1α, and a transcriptional coactivator common to both pathways, NFYC. Together, the ATF6 and IRE1 pathways serve to rescue the ER from an overload of unfolded proteins by increasing chaperone production and ER lipid biogenesis (Todd et al., 2008). Our screen also identified several members of the SEC61 and the HRD ligase protein translocation complexes (e.g., Derlin-1; Figure 1B). These proteins are critical for ER-associated degradation (ERAD), which helps rescue an unfolded protein burden by removing misfolded polypeptides from the ER and shuttling them to the 26S proteasome (Vembar and Brodsky, 2008).

The UPR and ERAD hits were particularly interesting because ER stress has been reported to be a defining feature of the tumor cell state, and components of these pathways are currently being pursued as cancer-specific targets for stand-alone treatment (Hetz, 2009; Wang et al., 2009). Thus, we performed secondary validation on ten hits within these pathways, using siRNA with targeting sequences distinct from those employed in the primary screens. To quantify sensitization, we infected RNAi-treated cells with increasing doses of Maraba virus and generated survival curves (Figure 1C). We then modeled the curves using nonlinear regression and determined the shift in the dose of virus required to kill 50% of the cells (EC_{50} shift). In all cases in which RNAi induced significant gene knockdown (nine of ten targets), U373 cells were significantly sensitized to virus-mediated killing (ranging from 1.4 to 3.7 log shifts in EC_{50}; Figure 1D, and representative images in Figure 1E). Although XBP1 did not emerge from our primary screen, given its critical function in mediating IRE1α-dependent transcription (Glimcher, 2010) we reevaluated it using RNAi duplexes distinct from those used in the primary screen. Indeed, these analyses demonstrated that, similar to *IRE1α* and our other UPR hits, *XBP1* depletion dramatically sensitized U373 cells to Maraba virus killing (EC_{50} shift, 3.2 logs, Figure 1D). To rule out off-target effects, we performed rescue experiments for ATF6α and IRE1α, which were chosen because they are not only representative ER stress response hits from the primary screen but also strong candidate druggable targets. Cells stably expressing murine ATF6α (mATF6α) were completely refractory to the

(C) U373 cells were treated with siRNA for 72 hr prior to Maraba virus infection, and viability assays were performed after 48 hr. The "EC_{50} shift" for cells silenced for *IRE1α* is depicted. M, mock infected.
(D) EC_{50} shifts (black bars, left y axis) were determined for U373 cells treated with Maraba virus (48 hr) following treatment with siRNA (72 hr) targeting a series of UPR/ERAD hits from the screen. Relative mRNA expression for each gene following siRNA knockdown (72 hr) is depicted in white (right y axis).
(E) Phase-contrast images of U373 cells treated first with siRNA (72 hr), followed by Maraba virus infection (moi 5; 24 hr). Scale bar, 100 μm.
(F) Cell viability assays were conducted 48 hr after Maraba virus infection, in U373 cells ectopically expressing mouse ATF6α (or control green fluorescent protein [GFP]) ± siRNA targeting human *ATF6α* (or nontargeting [NT] control; left panel) or human XBP1(s) (or control) ± siRNA targeting human *IRE1α* (or control; right panel). Western blots demonstrating gene silencing and ectopic gene expression are shown.
(G) Representative tumor and normal cell lines were treated with siRNA targeting *IRE1α* for 72 hr followed by Maraba virus. Cell viability assays were performed 48 hr later and EC_{50} shifts determined.
(H) Cell viability assays were performed on a panel of cancer-derived cell lines 48 hr after Maraba virus infection, which followed siRNA-mediated knockdown of *IRE1α* or *ATF6α* (72 hr).
(I) Cell viability was measured, and EC_{50} shifts were determined after 48 hr infection with wild-type (WT) or attenuate (MG1) Maraba virus (Brun et al., 2010) or VSV-WT, which followed 72 hr siRNA treatment.
For all experiments, $^*p < 0.05$; data shown as ±SD.
See also Tables S1 and S2.

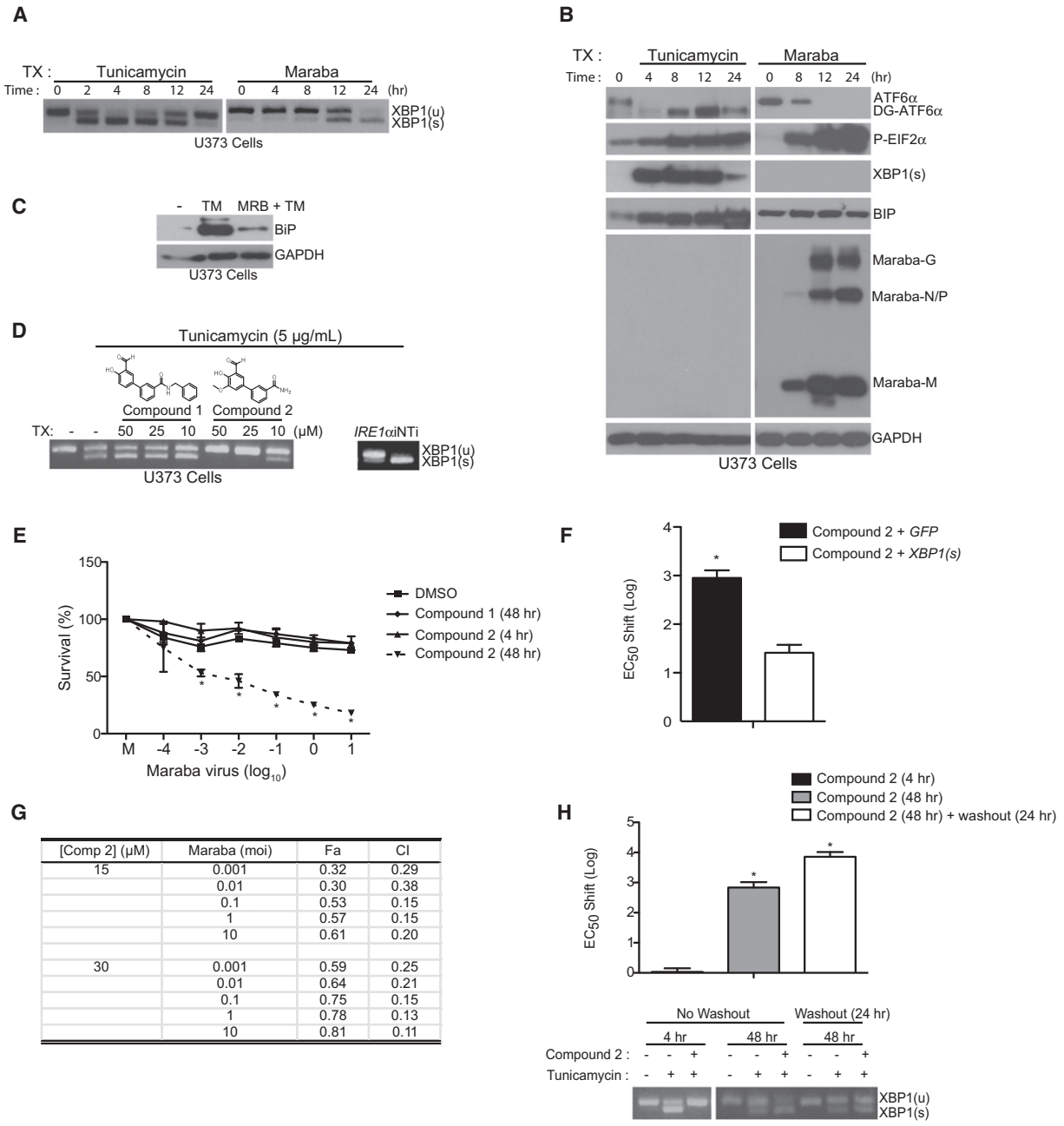

[Comp 2] (μM)	Maraba (moi)	Fa	CI
15	0.001	0.32	0.29
	0.01	0.30	0.38
	0.1	0.53	0.15
	1	0.57	0.15
	10	0.61	0.20
30	0.001	0.59	0.25
	0.01	0.64	0.21
	0.1	0.75	0.15
	1	0.78	0.13
	10	0.81	0.11

Figure 2. Synthetic Lethal Interaction between ER Stress Response Blockade and Rhabdovirus Infection Requires a Preconditioning Process

(A) U373 cells were treated with the ER stressor TM (5 μg/ml) or Maraba virus (moi 5). Total RNA was collected and RT-PCR for *XBP1* splicing performed.

(B) Cells were treated as in (A). Total cell lysates were collected and immunoblot analyses conducted (DG-ATG6α, deglycosylated ATF6α, due to the inhibitory effect of TM on glycosylation).

(C) U373 cells were untreated (–) or treated with TM (5 μg/ml; 24 hr) or Maraba virus (moi 5) for 6 hr prior to TM for 24 hr (MRB + TM). Total cell lysates were collected and immunoblots performed.

(D) U373 cells were treated with putative IRE1α small molecule inhibitors (2 hr) prior to TM treatment (4 hr). Total RNA was collected and RT-PCR performed. RNAi targeting *IRE1α* (72 hr) was used as a control (right panel).

(E) U373 cells were treated with compound 2 (50 μM) or controls for 4 or 48 hr prior to Maraba virus infection. Cell viability assays were performed 48 hr later. M, mock infected.

(F) U373 cells ectopically expressing XBP1(s) (or control) were treated with compound 2 (50 μM) for 48 hr prior to Maraba virus infection. Cell viability assays were performed 48 hr later.

(G) U373 cells were treated with compound 2 (48 hr) followed by Maraba virus (48 hr). Cell viability assays were conducted and combination index analyses performed.

synthetic lethal phenotype associated with Maraba virus infection and *hATF6α* knockdown (Figure 1F), whereas the sensitization phenotype induced by *IRE1α* knockdown was largely reversed in cells expressing constitutively active XBP1(s) (the product of the endonuclease activity of IRE1α; Figure 1F). Taken together, these experiments validate our primary screening result that Maraba virus-mediated oncolysis is greatly enhanced by knocking down components of the UPR and ERAD pathways.

To evaluate therapeutic index, we silenced *IRE1α* in a series of primary human cell lines (GM38 skin fibroblasts, normal human astrocytes [NHAs], and Wi38 lung fibroblasts) prior to rhabdovirus infection. In contrast to the pronounced sensitization observed in U373 glioblastoma cells, *IRE1α* knockdown had limited to no effect on Maraba virus-mediated killing of the normal cell lines (Figure 1G). We next examined the scope of the synthetic lethal phenotype in a representative subset of the NCI 60 tumor cell panel (Brun et al., 2010). RNAi-mediated knockdown of *IRE1α* or *ATF6α* significantly sensitized the majority of cancer cell lines tested to Maraba virus-mediated killing (Figure 1H). Moreover, oncolysis by the prototypic oncolytic rhabdovirus VSV (Stojdl et al., 2000b) and an engineered clinical candidate strain of Maraba virus (Maraba-MG1) (Brun et al., 2010) was similarly enhanced by UPR inhibition (Figure 1I). Collectively, these data suggest that the enhancement of rhabdovirus-mediated oncolysis conferred by inhibiting components of the ER stress response is tumor cell specific and may have widespread utility across a diverse range of tumor types.

Synthetic Lethal Interaction between ER Stress Response Blockade and Rhabdovirus Infection Requires a Preconditioning Process

VSV infection has recently been shown to cause ER stress (Liu et al., 2009), and thus, at first glance the most parsimonious mechanism to explain our synthetic lethal phenotype is an inadequate host cell response to virus-induced ER stress resulting in accelerated cell death. Indeed, Maraba virus infection caused noticeable ER stress in cancer cells, characterized by the activation of the upstream UPR sensors IRE1α (measured by *XBP1* mRNA splicing; Figure 2A), ATF6α (measured by its cleavage; Figure 2B), and PERK (measured by EIF2α phosphorylation; Figure 2B). However, as part of co-opting the host cell's synthetic machinery for the generation of viral progeny, rhabdoviruses are known to potently inhibit host gene expression by blocking mRNA transcription (Black and Lyles, 1992), nuclear to cytoplasmic mRNA shuttling and protein translation (Brun et al., 2010; Stojdl et al., 2000a, 2003). Therefore, not surprisingly, despite having strongly activated the UPR, a Maraba virus infection did not lead to elevated levels of the representative downstream UPR effector proteins XBP1(s) and BIP (Figure 2B). Moreover, the expression of BIP in response to the ER poison tunicamycin (TM) was dramatically blunted by a preceding infection with Maraba virus, further demonstrating that this rhabdovirus can actively block UPR gene expression in the face of ER stress (Figure 2C). Taken together, these results indicate that although a Maraba virus infection generates an ER stress that triggers the UPR-signaling cascade, it concomitantly blocks UPR-mediated gene expression, thereby rendering the response functionally inert. As such, an inadequate response to virus-induced ER stress is not responsible for the observed synthetic lethal interaction between rhabdovirus and UPR/ERAD knockdown because the UPR is already functionally inhibited upon rhabdovirus infection independently of external manipulation.

Because siRNA knockdown of UPR/ERAD targets was performed for up to 72 hr before virus was added to the cultures, we postulated that sustained inhibition during the siRNA knockdown period might be responsible for the sensitization observed. To test this idea, we synthesized a number of salicylaldehyde-based compounds that had been reported to inhibit IRE1α (Mannkind-Corporation, 2008) along with several variants of the original structure. We first measured their ability to inhibit *XBP1* splicing by IRE1α in a cell-based assay and found that several were effective in the micromolar range (representative subset depicted in Figure 2D). We then evaluated the most potent of these, designated compound 2, and found that it greatly enhanced rhabdoviral oncolysis in U373 cells when dosed for 48 hr (compound administered 48 hr and again 24 hr prior to virus infection, i.e., sustained inhibition), but not 4 hr (i.e., acute inhibition; Figure 2E). Importantly, drug-mediated sensitization significantly correlated with IRE1α inhibition (Figure S1), and ectopically expressed XBP1(s) significantly reduced the sensitization phenotype observed (Figure 2F). These data strongly suggest that IRE1α is indeed the functional target of compound 2, and are in agreement with a recent report demonstrating that this class of salicylaldehyde-based compounds directly and selectively inhibits the endonuclease activity of IRE1α (Volkmann et al., 2011). To determine whether the interaction between Maraba virus and IRE1α inhibition was synergistic or additive, we performed combination index experiments (Chou et al., 1994), which demonstrated that compound 2 interacted synergistically (CI < 1.0) with Maraba virus across a range of doses and multiplicity of infections (mois) (Figure 2G). In contrast we did not observe an interaction between the negative control compound 1 and Maraba virus at any dose across the same range (Figure 2E; data not shown). Finally, we sought to determine if the sensitization phenotype actually required IRE1α inhibition at the time of virus infection. For these experiments we treated U373 cells with compound 2 for 48 hr before washing the cells and adding new media (i.e., "washout") for another 24 hr prior to Maraba virus infection. Remarkably, the degree of sensitization was unaltered (Figure 2H, top panel) even after the drug was removed and IRE1α activity was restored (Figure 2H, bottom panel). In fact during the course of this experiment, we noticed that compound 2 was no longer inhibiting

(H) Top panel shows that U373 cells were treated with compound 2 (30 μM) for either 4 hr, 48 hr (dosed at t = −48 hr and −24 hr), or 48 hr, followed by a 24 hr "drug washout" period, and infected with Maraba virus. Cell viability assays were performed 48 hr post-virus infection and EC_{50} shifts determined. Bottom panel illustrates that U373 cells were treated with compound 2 (30 μM) (as described for top panel) prior to being treated with TM (5 μg/ml) for 4 hr. Total RNA was collected and RT-PCR performed for *XBP1* splicing.

For all experiments, *p < 0.05; data shown as ±SD. Fa, fractional effect; CI, combination index.

See also Figure S1.

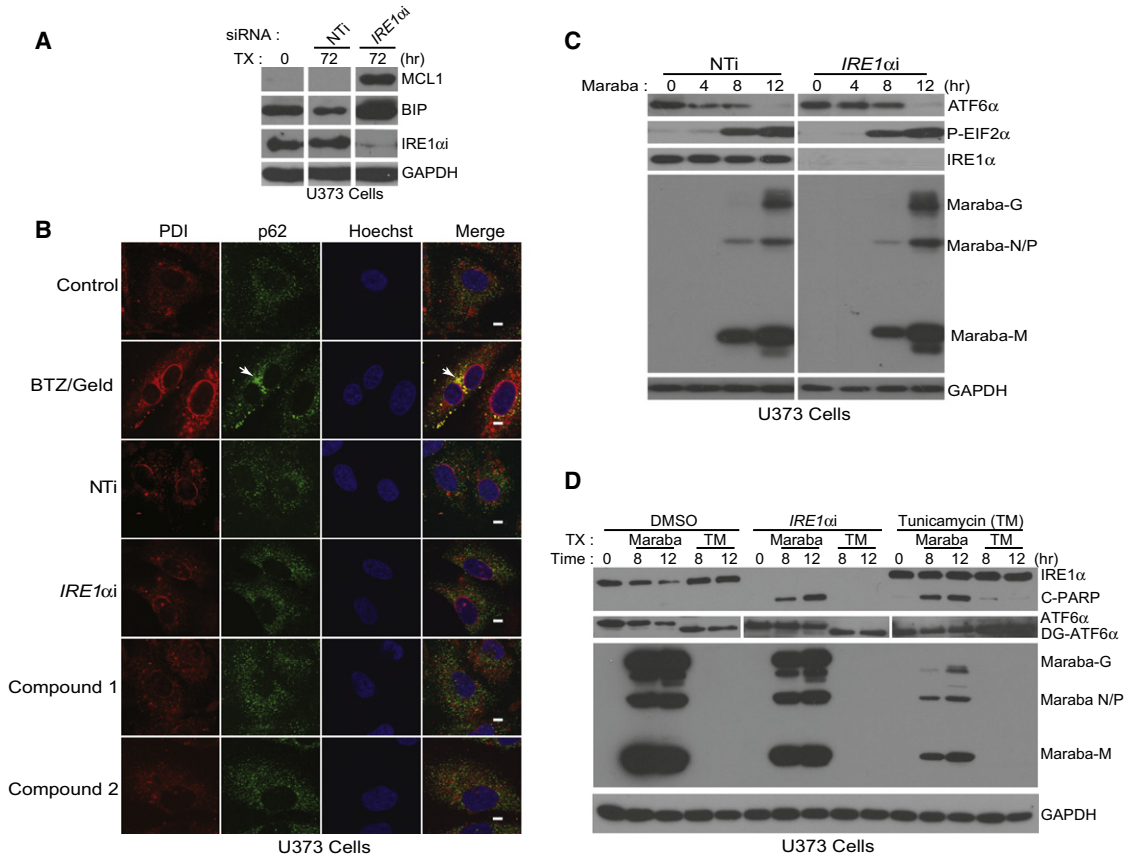

Figure 3. UPR Inhibition Leads to ER Preconditioning in Cancer Cells, which Sensitizes Them to Rhabdoviral Oncolysis

(A) U373 cells were treated with siRNA (72 hr), total cell lysates were collected, and immunoblots performed.

(B) U373 cells were treated as indicated with chemical ER stressors (bortezomib [25 nM]/Geldanamycin [120 nM]; compound 1 [30 μM], compound 2 [30 μM]) for 48 hr or treated with nontargeting or *IRE1α* targeting siRNA for 72 hr and then fixed and imaged for the protein aggregation marker p62. PDI is a marker for the ER, and Hoechst stains the nucleus. White arrow points to large foci of gross protein aggregation in positive control cells. Scale bars, 3 μm.

(C) Cells were treated with siRNA (72 hr), followed by infection with Maraba virus (moi 5). Total cell lysates were collected and immunoblots performed.

(D) Cells were treated as in (C) or treated with TM (5 μg/ml) for 24 hr followed by 24 hr "washout," after which cells were infected with Maraba virus (moi 5) or treated with TM (5 μg/ml). Total cell lysates were collected at the indicated time points and immunoblots performed.

See also Figure S2.

IRE1α activity 24 hr after it was added to the media, even without a washout. Collectively, these data demonstrate that the sensitization mediated by ER stress blockade and the triggering of cell death by virus infection are temporally separable events. This observation points toward a preconditioning process that durably alters the tumor cell's response to a subsequent rhabdovirus infection.

ER Preload Rewires Cancer Cells for Caspase-2-Dependent Apoptosis

Many cancer cells accumulate unfolded proteins as a function of their malignant nature (Moenner et al., 2007). Therefore, we postulated that inhibiting a component of the ER stress response might gradually lead to an unfolded protein burden in the ER of cancer cells, which would predispose them to ER stress-mediated apoptosis in response to a subsequent rhabdovirus infection. Indeed, we found that cells treated with RNAi targeting *IRE1α* for 72 hr had increased levels of both BIP and MCL1 protein (Figure 3A), which are each known to be transcriptionally induced following ER stress independently of IRE1α. These data demonstrate that sustained inhibition of IRE1α in tumor cells leads to a sufficiently large ER protein burden as to trigger a UPR, and this was not observed in normal cells (Figure S2A). However, immunostaining for ubiquitin or p62 revealed no gross protein aggregation following *IRE1α* knockdown or compound 2 treatment (Figure 3B; Figure S2B). We also did not detect any evidence of an active ER stress response at this time of virus infection because early markers of UPR activation (EIF2α phosphorylation and ATF6α cleavage) were indistinguishable between control and *IRE1α* siRNA pretreated tumor cells (Figure 3C, 0 hr). Moreover, loss of *IRE1α* had no effect on the magnitude or kinetics of UPR activation following Maraba virus infection (Figure 3C), suggesting that the capacity of the tumor cell to respond to an unfolded protein burden was not diminished at the time of virus infection. Collectively, these data suggest that the protein load induced upon genetic knockdown or chemical inhibition of IRE1α was transient, having likely been sufficiently managed by the other arms of the UPR it evoked.

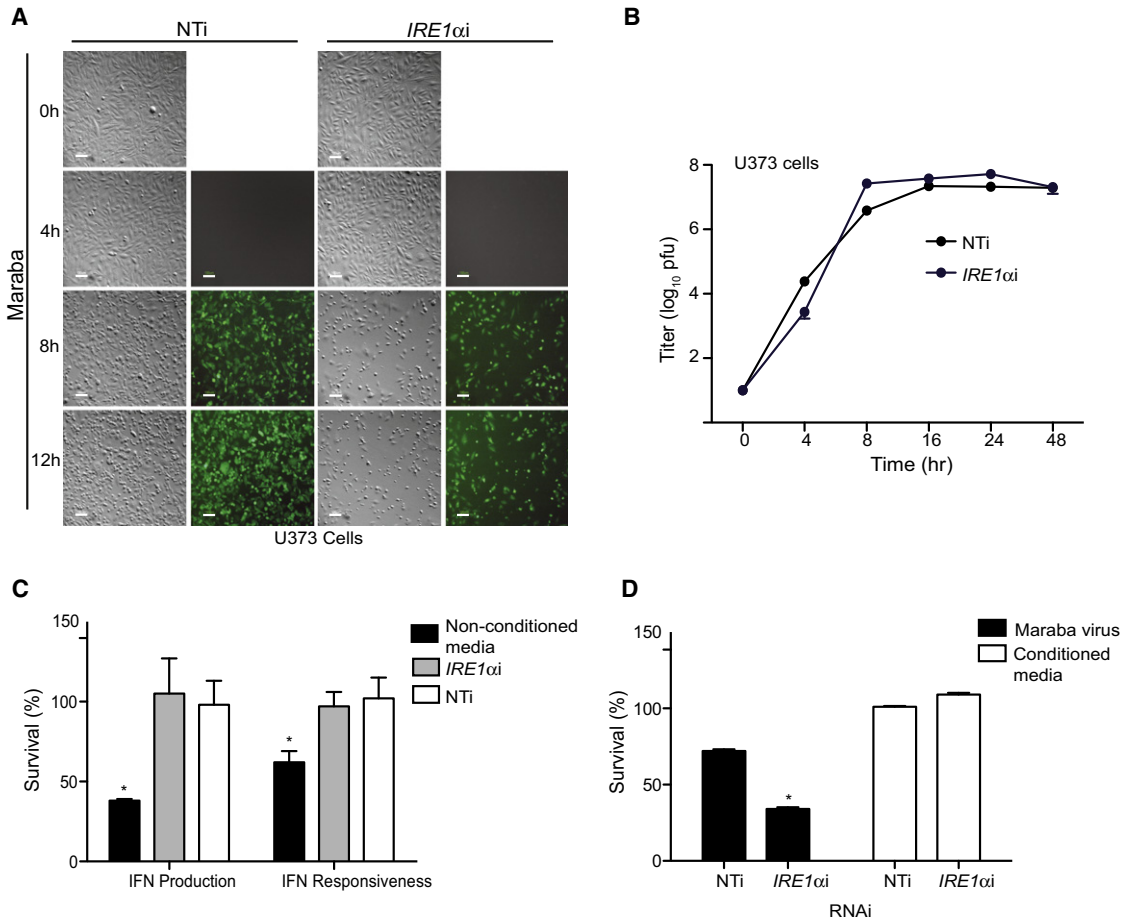

Figure 4. ER Preconditioning Has No Bearing on Rhabdovirus Infectivity, Productivity, or the Ability to Secrete or Respond to Interferons, and Does Not Lead to "Bystander Killing"

(A) U373 cells were treated with siRNA (72 hr) prior to Maraba infection (moi 5), and phase-contrast and fluorescent microscopy images were captured following infection. Scale bars, 100 μm.

(B) U373 cells were treated as in (A), and single-step growth analyses conducted.

(C) Production: Ovcar-4 cells treated with siRNA targeting *IRE1α* (or nontargeting (NT)) RNAi for 72 hr were infected with VSV-Δ51 (Stojdl et al., 2003) for 18 hr, at which time the conditioned media were collected and virus neutralized. Conditioned media (gray and white bars) or nonconditioned media (complete DMEM as a control; black bars) were then added to Vero cells for 24 hr prior to Maraba virus infection. After 48 hr infection, viability assays were performed. Responsiveness: conditioned media were generated from PC3 cells infected with VSV-Δ51 for 18 hr. Conditioned media were then added to OVCAR-4 cells that had been treated with siRNA targeting *IRE1α* or NT (72 hr) (gray and white bars), or nonconditioned media (black bars) were added to untreated OVCAR-4 cells as a control. After 24 hr, cells were infected with Maraba virus for 48 hr and viability assays performed.

(D) Black bars (control experiments) indicate U373 cells that were treated with non (NT)- or *IRE1α*-targeting siRNA prior to infection with Maraba virus (moi 10). White bars (bystander experiments) show U373 cells that were infected with Maraba virus (moi 10), and after 24 hr infection, the conditioned media were collected and transferred onto U373 cells that had been previously treated with NT- or *IRE1α*-targeting RNAi. Cell viability was assessed after 72 hr.

For all experiments, $^*p < 0.05$; data shown as ±SD.

As a compliment to these studies, we induced ER preload by treating cells with either RNAi targeting *IRE1α* or pulsing them with a dose of the strong ER stress inducer TM, and evaluated how the cells responded to a further ER insult by treating them with a second dose of TM. In these experiments we found that the preloaded cells were able to respond to the second ER stressor with similar kinetics and dynamics as compared to naive cells (Figure 3D, ATF6α blots, lanes 9–10 versus 4–5). Importantly, this further ER stress did not trigger cell death (Figure 3D, PARP blot, lanes 9–10 and 14–15 versus 7–8 and 12–13). Taken together, these data demonstrate that IRE1α inhibition does not sensitize cancer cells toward rhabdovirus-mediated killing as a result of diminished capacity to deal with virus-induced ER stress.

Thus, we postulated that it is a response to ER stress prior to virus infection rather than ER stress per se that is the sensitizing agent. We first asked whether ER preload affected any aspect of the virus life cycle in cancer cells. We noted that UPR inhibition had no bearing on viral protein expression following a Maraba virus infection (Figures 3C and 3D), and further experiments confirmed that knocking down *IRE1α* did not alter the infectivity (Figure 4A) or productivity (Figure 4B) of Maraba virus in cancer cells. These data demonstrate that transient ER stress does not affect the life cycle of Maraba virus. It is well established that

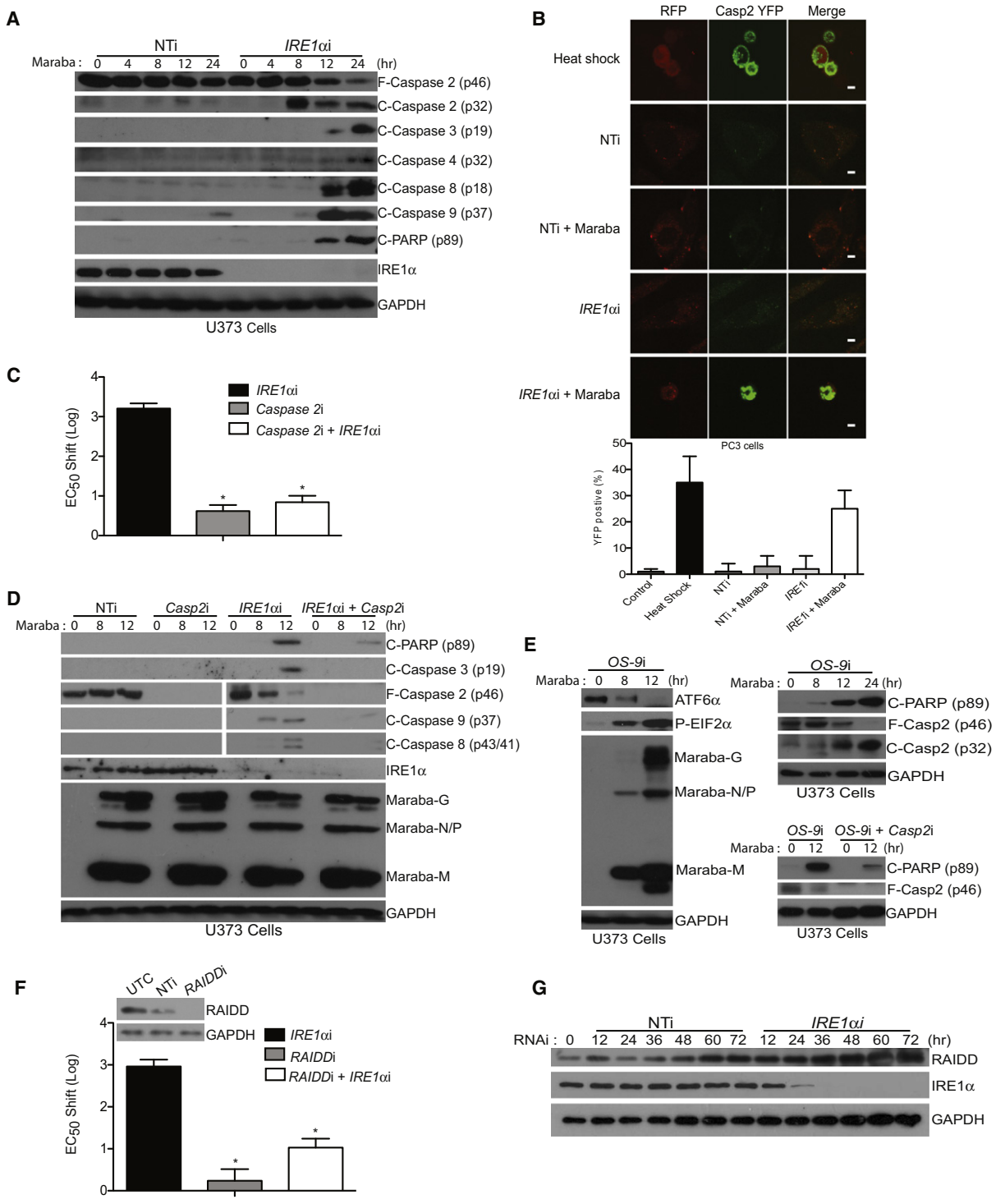

Figure 5. ER Preconditioning Rewires Cancer Cells for Caspase-2- and RAIDD-Dependent Apoptosis in Response to Rhabdovirus Infection

(A) U373 cells were treated with siRNA (72 hr), followed by infection with Maraba virus (moi 5). Total cell lysates were collected and immunoblots performed.

(B) In the top panel, PC3 cells were treated for 24 hr with siRNA as indicated and then transfected with Casp2-CARD VC, Casp2-CARD VN, and pmKATE2 (RFP transfection control). Twenty-four hours later, cells were either left untreated or infected with Maraba virus (moi = 5). Positive control cells were heated for 1.5 hr at 44°C (heat shock). Cells were assessed 8 hr after virus treatment for the percentage of cells that were Venus positive (green). Scale bars, 3 μm. Bottom panel is a histogram (top panel) with quantified caspase-2 activation denoted as the percentage of transfected cells that showed YFP complementation. A minimum of 200 cells per well from 24 replicate wells was counted.

(C) Cells were treated with siRNA (72 hr), followed by infection with Maraba virus across a 6-log dose range. After 48 hr, cell viability was measured, and EC_{50} curves were plotted.

rhabdoviruses, including Maraba virus, are exquisitely sensitive to the human innate immune system via type I interferon signaling (Müller et al., 1994). Interferons are protective cytokines that are processed in the ER/Golgi system before being secreted to warn neighboring cells of an impending virus encounter. These cytokines signal through the type I interferon receptor (IFNR1), which is also processed in the ER/Golgi system. Previous work has shown that ER stress can inhibit proper IFNR1 processing in the ER/Golgi system, which leads to IFNR1 depletion and enhanced susceptibility to a rhabdovirus infection (Liu et al., 2009). Thus, we asked whether transient ER stress could alter a cancer cell's ability to secrete interferon in response to a rhabdovirus infection, or to respond to interferon secreted by neighboring cells. Using an interferon bioassay, we found that silencing *IRE1α* in OVCAR-4 cells (which have an intact interferon system) had no bearing on their ability to secrete or respond to interferon cytokines (Figure 4C). These data demonstrate that UPR inhibition does not induce an interferon defect in cancer cells in our assay system. Finally, we asked whether transient ER stress could sensitize cancer cells toward death induced by other cytokines secreted upon Maraba virus infection (e.g., TNFα), the so-called "bystander effect." We did not detect any cytotoxicity when conditioned media from virus-infected U373 cells were transferred to U373 cells that had been previously treated with either non- or *IRE1α*-targeting RNAi (Figure 4D).

Thus, we hypothesized that a transient ER stress might rewire the cancer cell's signaling networks toward increased cell death upon subsequent oncolytic virus challenge. Indeed, *IRE1α* knockdown greatly enhanced the kinetics of apoptosis during Maraba virus infection, as measured by the cleavage of PARP and members of the caspase cascade (Figure 5A). Notably, caspase-2 was strongly activated in tumor cells (but not normal cells) early after virus infection only when *IRE1α* was knocked down (Figure 5A; Figure S3A). Bimolecular fluorescent complementation analyses of caspase-2 activation by induced proximity (Bouchier-Hayes et al., 2009) confirmed that caspase-2 was strongly activated in response to combined IRE1α inhibition and Maraba virus infection (Figure 5B; Figure S3B). Caspase-2 is an initiator caspase that has been implicated in several stress-mediated apoptotic cascades, such as those emanating from DNA damage (Vakifahmetoglu-Norberg and Zhivotovsky, 2010) as well as ER stress (Cheung et al., 2006). To examine the relevance of caspase-2 activation, we knocked it down simultaneously with *IRE1α* and measured apoptosis following Maraba virus infection. In these experiments *caspase-2* knockdown almost completely rescued the synthetic lethal interaction between *IRE1α* knockdown and virus infection (Figures 5C and 5D). Qualitatively similar caspase-2 rescue data were obtained when cells were rendered null for the ERAD component OS-9 (Figure 5E). Consistent with the observation that caspase-2 was activated early following a virus infection in cells treated with RNAi targeting *IRE1α*, *caspase-2* knockdown inhibited the activation of the activator caspases 8 and 9 as well as the downstream effector caspase 3 following a virus infection in cells treated with *IRE1α* siRNA. Collectively, these data suggest that a transient ER stress preconditions cancer cells to commit caspase-2-dependent apoptosis in response to a subsequent Maraba virus infection.

We next asked whether caspase-2 itself senses ER preload in response to UPR inhibition, or whether the link from ER preload to caspase-2 lies upstream. By western blotting, immunostaining, and bimolecular fluorescence complementation (BiFC) analyses, we have been unable to detect any changes in caspase-2 levels, localization, activation, or phosphorylation status during the preload period (data not shown). This suggests that whereas caspase-2 is central to sensitization, it itself is not directly responsive to ER stress during the preload period. However, when we examined the known caspase-2-interacting proteins PIDD and RAIDD, we found that whereas PIDD was dispensable for sensitization (Figure S3C), *RAIDD* knockdown largely rescued IRE1α knockdown-induced sensitization (Figure 5F). Moreover, RAIDD protein levels markedly increased throughout an ER preload period generated by RNAi targeting *IRE1α* (Figure 5G) and by compound 2 (Figure S3D), beginning at about the time cells become sensitized. Taken together, these data demonstrate that ER preload-mediated rewiring for caspase-2-dependent apoptosis upon viral infection is dependent on the adaptor protein RAIDD. Given these findings, we asked whether other stressors that have been shown to induce caspase-2- and RAIDD-mediated apoptosis are similarly enhanced by ER preload. Indeed, we found that both genetic and chemical inhibition of the UPR and/or ERAD dramatically sensitized tumor cells to killing by the DNA-damaging agent doxorubicin, a phenotype that was dependent on both RAIDD and PIDD (Figures S3E–S3H). These data appear to indicate that ER preload alters cell signaling upstream of caspase-2 in such a way as to generically sensitize to a number of caspase-2 activation complexes initiated from disparate triggers (proposed model depicted in Figure 6).

UPR Inhibition Potentiates Oncolytic Therapy in Primary Patient Samples and a Preclinical Model of Cancer

To evaluate the clinical relevance of this therapeutic strategy, we examined whether compound 2 pretreatment could sensitize freshly derived patient tumor samples to Maraba virus-mediated oncolysis. Cell cultures isolated from three patients with primary glioblastoma multiforme were treated with compound 2 for 48 hr prior to Maraba virus infection, and 48 hr later, viability assays demonstrated that each was significantly sensitized toward death (Figure 7A).

We next sought to evaluate the efficacy in several animal models of cancer. To begin, we undertook maximum tolerable

(D) Cells were treated with siRNA (72 hr), followed by infection with Maraba virus (moi 5). Total cell lysates were collected and immunoblots performed.
(E) Cells were treated with siRNA targeting OS-9 (±caspase-2i) for 72 hr followed by Maraba virus for 48 hr, and western blots were performed.
(F) Cells were treated with siRNA (72 hr), followed by infection with Maraba virus across a 6-log dose range. After 48 hr, cell viability was measured, and EC_{50} curves were plotted.
(G) Cells were treated with siRNA (72 h), followed by infection with Maraba virus (moi 5). Total cell lysates were collected and immunoblots performed.
For all experiments, *$p < 0.05$; data shown as ±SD.
See also Figure S3.

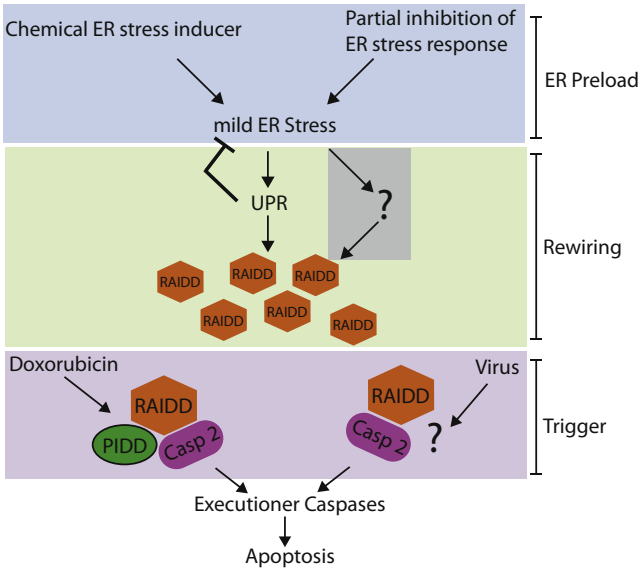

Figure 6. ER Preload Rewires Cancer Cells for Caspase-2 and RAIDD-Dependent Viral Oncolysis

Partial UPR (or ERAD) inhibition or treatment with a chemical ER stress inducer (e.g., TM) leads to a mild ER stress in cancer cells (ER Preload). As a result, a corrective UPR is activated, and RAIDD protein levels are increased (Rewiring). In response to a subsequent virus infection (or DNA-damaging agent), caspase-2 is activated eccentrically due to the increased surface area with which to seed induced proximity (Trigger), and apoptosis ensues.

dose (MTD) and pharmacokinetic (PK) studies of compound 2 in CD-1 nude mice. These experiments showed that a single dose of up to 1000 mg/kg of compound 2 was tolerated, had a half-life of >6 hr, and had properties consistent with efficient biodistribution to the extravascular tissues (Figure S4). To validate our combination therapy approach, we chose a chemoresistant (Boettcher et al., 2010; Hamilton et al., 1983) orthotopic OVCAR-4 xenograft model (Louie et al., 1985) that is also refractory to OVT. OVCAR-4 cells stably expressing firefly luciferase were injected intraperitoneally (i.p.) into CD-1 nude mice. We monitored tumor growth using in vivo optical imaging, and initiated treatment during the growth phase. To induce ER preconditioning, we treated animals with compound 2 for 3 days prior to the first virus injection. Consistent with our findings in cell culture, combination therapy dramatically reduced tumor burden in animal models, an effect that was sustained for >30 days with negligible tumor regrowth (Figures 7B and 7C). In contrast, rapid regrowth occurred after an early period of tumor regression using either virus or compound 2 alone.

As a complement to these experiments in human xenografts, we sought to test this treatment regimen in an immune-competent rodent tumor model. In vitro testing determined that the EMT6 breast cancer line, which is particularly resistant to stand-alone rhabdovirus therapy, was significantly sensitized to oncolytic virus killing when pretreated with compound 2 (Figure 7D). Using these cells to generate a tumor model, we confirmed that neither drug nor virus had an appreciable effect on tumor growth as single agents; however, combination therapy significantly reduced tumor burden (Figure 7E). Extending compound 2 treatment to more than 12 days in combination with virus treatment continued to increase efficacy (Figure 7F). Taken together, these data demonstrate proof of concept that modulating the ER stress responses can be exploited to enhance OVT in vivo. We anticipate that the ongoing development of more clinically relevant nanomolar compounds and/or simultaneous targeting of multiple components of the ER stress response may provide even greater boosts in efficacy.

DISCUSSION

Using a genome-wide RNAi-screening approach, we have discovered that inhibiting the ER stress response preconditions cancer cells to undergo caspase-2-dependent apoptosis when subsequently challenged with an oncolytic rhabdovirus. This exploitation of the host/virus interaction increased the potency of oncolytic Maraba virus cytotoxicity by up to 10,000-fold throughout a diverse range of tumor-derived cell lines, without increasing toxicity in normal cells. To validate ER preload as a clinically relevant therapeutic strategy, we show that UPR inhibition can sensitize primary patient glioblastoma tumors to Maraba infection. Moreover, we demonstrate that this combination strategy can improve the effectiveness of oncolytic Maraba virus in both an immunocompetent mouse model and an immunodeficient human xenograft model of cancer. This provides an additional mechanism by which oncolytic viruses can selectively target tumor cells and serves to further increase the therapeutic index of this class of experimental cancer therapy. We are currently working to identify more potent IRE1α inhibitors and exploring the use of multiple UPR/ERAD inhibitors to further enhance the effectiveness of this combination strategy.

We also show that the sensitization of tumor cells to Maraba virus is dependent on a cellular response to a transient ER stress, but not a concurrent one. This response leads to the predisposition toward a caspase-2-mediated apoptotic death pathway. We are currently pursuing both the mechanism by which ER preload is able to prime a caspase-2 response in tumor cells, as well as the means by which rhabdoviruses and other stressors can subsequently trigger this response to kill cells. Currently, it has been established that caspase-2 activation can occur through both PIDD-dependent and independent mechanisms (Tinel and Tschopp, 2004) (Manzl et al., 2009). Our data suggest that the PIDDosome is not involved in virus-mediated activation of caspase-2 following ER preload but is involved in its activation by doxorubicin (Figure S3). This seems to indicate that ER stress alters cell signaling upstream of PIDD and that ER preload can generically sensitize to a number of caspase-2 activation complexes initiated from disparate triggers. Consistent with this model, we have found that RAIDD is required for sensitization and that its protein content is markedly elevated in response to ER preload. It may be that RAIDD is upregulated during UPR and/or ERAD responses and that this would help prepare the cell for the decision to commit apoptosis should the UPR/ERAD not be sufficient to resolve the damage. Experiments are currently ongoing to identify more of the components of this potent synthetic lethal signaling pathway.

Our study establishes a successful strategy for the rational design of ''chemical-biological combination therapies'' using functional genomic screening for host/virus interactions.

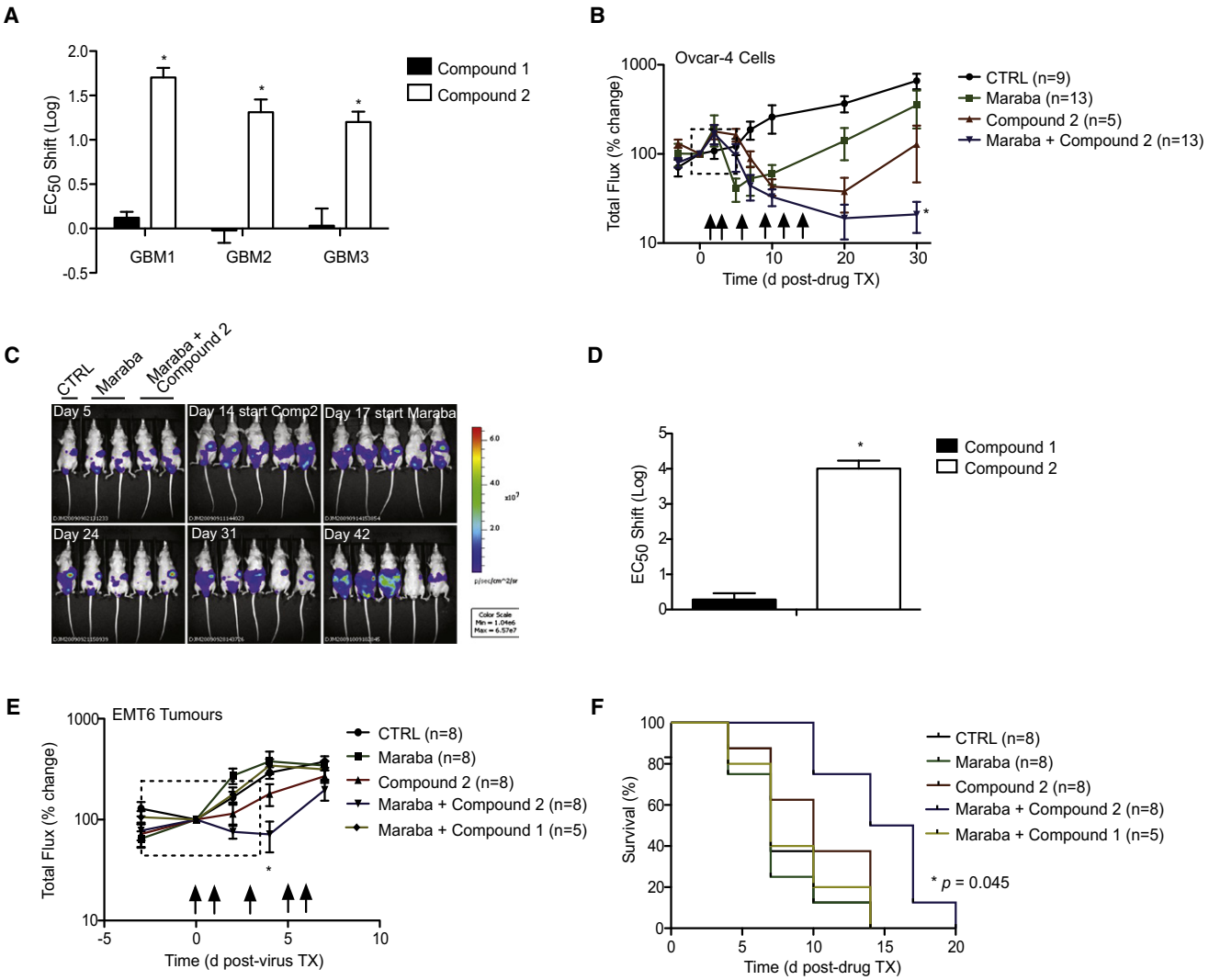

Figure 7. Inhibiting IRE1α Enhances Oncolytic Therapy in Patient Tumor Samples and Murine Cancer Models

(A) Cells isolated from three patients with glioblastoma multiforme were treated with compound 1 or 2 (15 μM) or DMSO control for 48 hr, followed by Maraba virus across a 6-log dose range. Cell viability assays were performed 48 hr later and EC_{50} shifts determined (plotted relative to DMSO control).

(B) Luciferase-tagged OVCAR-4 cells ($5e^6$) were delivered i.p. into CD-1 nude mice. At day 14, mice were treated twice daily with compound 2 (250 mg/kg; i.p. delivery) or vehicle for 6 consecutive days (drug TX window is outlined by the dotted lines). Maraba-MG1 treatment ($1e^5$ PFU; IV injections) was initiated 48–72 hr later (virus injections depicted by arrows). Tumors were regularly evaluated using IVIS bioluminescent imaging. The graph depicts relative change in luminescent signal, which corresponds to tumor size.

(C) Representative bioluminescent images from (B).

(D) EMT6 cells were treated with compound 1 or 2 (50 μM) or DMSO control for 48 hr prior to Maraba virus infection across a 6-log dose range. Viability assays were conducted 48 hr later and EC_{50} shifts determined (plotted relative to DMSO).

(E) Luciferase-tagged EMT6 cells ($1e^5$) were implanted into the breast fat pads of Balb/c mice. Compound 1 or 2 or PBS treatment was initiated at day 7 (250 mg/kg; i.p.; twice daily for 6 days; treatment window depicted by the dotted box). Maraba-DM injections ($1e^7$ PFU; IV) commenced on day 10 (black arrows). Bioluminescent data are plotted (as above).

(F) Kaplan-Meier curve depicting mouse survival in an EMT6 model. The experiment was done as in (E), except that compound 1 and 2 treatments were extended for an additional 6 days.

For all experiments, *$p < 0.05$; data shown as ±SD.

See also Figure S4.

Although other chemovirus combination therapies have been reported, with enhancements to oncolytic efficacy (Ottolino-Perry et al., 2010), our study demonstrates the utility of genome-scale systematic analyses of host/virus interactions to identify unpredicted synergies. This study adds to the breadth of opportunities for combinations beyond those predicted by our current molecular understanding of host/tumor/virus interactions. For example whereas it is known that rhabdoviruses induce UPR (Liu et al., 2009) and that UPRs are largely transcriptional, vesiculoviruses such as VSV and Maraba virus are known to block host

transcriptional responses, and we show here that UPR is effectively nullified during a normal virus infection of mammalian cells. Therefore, it would not be predicted that further inhibition of this pathway would be a fruitful avenue for a combination therapy. Yet, our screens identified a host pathway that robustly modulates rhabdovirus cytotoxicity through an unconventional mechanism of action where the cellular response to an ER stress, and not the stress itself, is the critical component of oncolytic synergy.

Finally, it is noteworthy that rhabdoviruses are currently in clinical development (D.F.S., unpublished data), whereas UPR (Hetz, 2009) and ERAD (Wang et al., 2009) inhibitors are being actively pursued for cancer treatment. Our data suggest that these agents will act synergistically when used in combination, and support their evaluation in the clinical setting.

EXPERIMENTAL PROCEDURES

RNAi Screening

An arrayed library of siRNA pools (Dharmacon, Thermo Fisher Scientific, Lafayette, CO, USA) was used to target ~18,200 human genes in OVCAR-8 (ovarian carcinoma), U373 (glioblastoma), or NCI-H226 (nonsmall cell lung carcinoma) cells. Tumor cells were seeded in 384-well plates (OVCAR-8, 1250 cells/well; U373, 625 cells/well; NCI-H226, 625 cells/well). Each plate had additional control wells with a nontargeting control siRNA (Dharmacon nontargeting Pool #2) to measure the effect of siRNA transfection on infection, and siRNA targeting *plk-1* (Dharmacon) was used to monitor knockdown efficiency. Quadruplicate plate sets were reverse transfected with siRNA (10 nM) using RNAimax (Invitrogen, USA) and incubated for 72 hr. From these, duplicate sets of plates were either mock infected or infected with wild-type Maraba virus (moi: OVCAR-8, 0.1; U373, 0.05; NCI-H226, 0.1). Infections were incubated for 48 hr (OVCAR-8) or 72 hr (U373 and NCI-H226), after which resazurin dye (20 μg/ml) was added to each well, incubated for 6 hr, and assayed for absorbance (573 nm) to score cell viability.

In Vitro Cytotoxicity Assays with RNAi and Determination of "EC_{50} shifts"

Cells were seeded onto 96-well plates to a confluence of ~50%. The following day, siRNA transfections were performed, and 72 hr later, the cells were infected at log 10 dilutions with wild-type Maraba virus (except for Figure 1G, which used the indicated viruses). After 48–72 hr of infection (depending on the cell line), Resazurin sodium salt (Sigma-Aldrich) was added to a final concentration of 20 μg/ml. After a 6 hr incubation, the absorbance was read at a wavelength of 573 nm. To determine the EC_{50}, kill curves were modeled using nonlinear regression analysis (GraphPad Prism Software) and EC_{50} values determined. The EC_{50} shift was calculated by subtracting the EC_{50} of UPR targeted from nontargeted cell lines, and is represented as log 10 values.

XBP1-Splicing Assays

For qualitative analyses, total RNA was extracted from cells using a standard RNeasy spin column kit, as described by the manufacturer (QIAGEN). RNA was reverse transcribed to cDNA using SuperScript II RT (Invitrogen) following the manufacturer's guidelines. Standard PCR was performed using the following primers: XBP1-F, 5′-cct tgt agt tga gaa cca gg-3′; XBP1-R, 5′-ggg gct tgg tat ata tgt gg-3′. The PCR products were run out on a 3% agarose gel and visualized with UV imager. Images were scanned, and densitometry was performed using Scion Image software. For quantitative analyses, total RNA was extracted (as above), and real-time quantification was performed with Taqman One-Step RT-PCR Master mix reagents (Applied Biosystems) using the following primers and probes: forward primer 5′-AAGCCAAGGGGAATGAAGT-3′, reverse primer 5′-CCAGAATGCCCAA CAGGATA-3′; XBP1(u) probe, 5′-56-FAM-AGCACTCAGACTACGTGCACCT-3IABkFQ-3′, XBP1(s) probe 5′-56-JOE-CTGAGTCCGCAGCAGGTGCAGG-3IABkFQ-3′.

Protein Aggregate Formation

For protein aggregation imaging, cells were cultured in 384-well optical imaging plates (Aurora Biotechnologies, Carlsbad, CA, USA) and subjected to either chemical or genetic ER stressor as indicated for 48–72 hr, respectively. Cells were fixed with 4% formaldehyde, stained, and imaged in PBS at room temperature. Images were collected using a confocal microscope (FluoView 1000D; Olympus Inc.) equipped with a 60× water immersion 1.2 NA objective and processed using the Fiji distribution of ImageJ (http://fiji.sc/wiki/index.php/Fiji). P62 was detected using rabbit polyclonal antisera (Cell Signaling Technology; #5114) and anti-rabbit Alexa 488 (Invitrogen). Ubiquitin was detected using rabbit polyclonal antisera (Cell Signaling Technology; #3933) and anti-rabbit Alexa 488. The ER marker PDI was stained using the mouse monoclonal antibody RL77 (Thermo, USA). Cells were stained with Hoechst 33342 to visualize nuclei. All images were acquired at 100 μs/pixel at 512 × 512 pixel resolution with 3 pass Kalman filter processing.

Caspase-2 BiFC

To measure caspase-2 activation by induced proximity, we employed a caspase-2 BiFC system (Bouchier-Hayes et al., 2009). Cells were reverse transfected in 384-well format with siRNA targeting *IRE1α* or a nontargeting control siRNA. Twenty-four hours later, cells were forward transfected with a mixture of 10 ng of Casp2 CARD VN, 10 ng Casp2 CARD VC, and 5 ng pmKATE2 (RFP; Evrogen, Moscow) using FuGENE HD (Roche, USA). After 24 hr, cells were either mock infected or infected with Maraba virus at an moi of 5. Alternatively, an additional plate of cells was exposed to 44°C heat shock for 90 min and returned to the incubation as a positive control for caspase-2 activation. Following 8 hr of virus infection (or post-heat shock), cells were fixed in 4% formaldehyde and stained with Hoechst 33342 to visualize nuclei. Plates were imaged using an OPERA high-throughput confocal microscope (PerkinElmer, USA) using a 40× water immersion objective. Image analysis and quantification were performed using Acapella software (PerkinElmer).

Small Molecule Screening

U373 cells were plated in 6-well format to a confluence of ~75%. The following day, candidate small molecules were dissolved in DMSO and added directly to the cell culture media at a range of concentrations. After 2 hr, TM (5 μg/ml) was added, and total RNA was collected 4 hr later. RNA extraction and RT-PCR for *XBP1* splicing were performed as described above.

In Vitro Cytotoxicity Assays with Small Molecules

Cells were seeded onto 96-well plates to a confluence of ~50%. The following day, siRNA transfections were performed, or small molecule IRE1α inhibition was initiated. For the small molecules, DMSO was used as a vehicle with a drug concentration of 20–50 μM. Drug treatment occurred for either 4 hr ("acute" treatment), or was reapplied at 24 hr and left for 48 hr total ("sustained" treatment). Following knockdown or chemical inhibition, the cells were infected at log dilutions with the indicated rhabdoviruses. After 48–72 hr of infection (depending on the cell line), Resazurin sodium salt was added to a final concentration of 20 μg/ml. After a 6 hr incubation, the absorbance was read at a wavelength of 573 nm.

Ovarian Xenograft Model

Human ovarian carcinoma-derived OVCAR-4 cells, adapted for bioluminescent imaging, were injected into 6- to 8-week-old athymic CD-1 nude mice (i.p. injection, 5×10^6 cells per mouse). Untreated animals developed measurable abdominal tumors (assessed by IVIS imaging) by 4–7 days, became icteric by 3–4 months, and had to be euthanized shortly thereafter due to systemic disease, as characterized by enlarged cancerous liver and spleen, pale kidneys, and cancerous lymph nodes on the abdominal mesentery. For efficacy experiments, compound 2 (250 mg/kg; or vehicle [10% Tween 80]) was administered twice daily (i.p. injections), beginning on day 14 and ending on day 19. Maraba-MG1 (1×10^5 pfu per cell) or PBS was injected IV (tail vein) on days 16, 17, 19, 23, 25, and 27. Animals were monitored daily for weight loss, morbidity, hind leg paralysis, and respiratory distress. Tumor images were captured twice weekly with a Xenogen 200 IVIS system (Caliper LS, USA), and total luminescent flux was analyzed on computerized software (Xenogen). All animal experiments were approved by the University of Ottawa

Animal Research Ethics Board and carried out in accordance with guidelines of the National Institutes of Health and the Canadian Council on Animal Care.

Glioblastoma Patient Samples

Clinical samples were used in accordance with research ethics board approval from the Institutional Ethics Board at the Montreal Neurological Institute and Hospital (Montreal, Canada). Written informed consent was obtained for all patient samples in this study.

Statistical Analyses

For all statistical analyses except survival curves, one- and two-way ANOVAs were performed, followed by a Bonferroni multiple comparison's post hoc test to derive p values (GraphPad Prism Software). For survival curves, Mantel-Cox log rank analysis was used to compare plots (GraphPad Prism). For all tests, statistical significance was defined as $p < 0.05$.

SUPPLEMENTAL INFORMATION

Supplemental Information includes Supplemental Experimental Procedures, four figures, and two tables and can be found with this article online at doi:10.1016/j.ccr.2011.09.005.

ACKNOWLEDGMENTS

We kindly thank A.E. MacKenzie and R. Screaton for critically reading the manuscript, D. Green for his caspase-2 BiFC plasmid system, E. Brown for anti-VSV antibody, J.S. Diallo for help with the combination index analyses, and K. Petrecca for primary patient samples. D.F.S. is supported by the National Cancer Institute of Canada (NCIC), the Ontario Institute for Cancer Research (OICR), the Terry Fox Foundation, the Canadian Foundation for Innovation (CFI), Ontario Research Fund, Ottawa Regional Cancer Foundation, the Angels of Hope Foundation, the CHEO Foundation, and the Honey Badger Innovation Project.

Received: April 23, 2011
Revised: August 2, 2011
Accepted: September 13, 2011
Published: October 17, 2011

REFERENCES

Balachandran, S., and Barber, G.N. (2000). Vesicular stomatitis virus (VSV) therapy of tumors. IUBMB Life *50*, 135–138.

Black, B.L., and Lyles, D.S. (1992). Vesicular stomatitis virus matrix protein inhibits host cell-directed transcription of target genes in vivo. J. Virol. *66*, 4058–4064.

Boettcher, M., Kischkel, F., and Hoheisel, J.D. (2010). High-definition DNA methylation profiles from breast and ovarian carcinoma cell lines with differing doxorubicin resistance. PLoS One *5*, e11002.

Bouchier-Hayes, L., Oberst, A., McStay, G.P., Connell, S., Tait, S.W., Dillon, C.P., Flanagan, J.M., Beere, H.M., and Green, D.R. (2009). Characterization of cytoplasmic caspase-2 activation by induced proximity. Mol. Cell *35*, 830–840.

Breitbach, C.J., Paterson, J.M., Lemay, C.G., Falls, T.J., McGuire, A., Parato, K.A., Stojdl, D.F., Daneshmand, M., Speth, K., Kirn, D., et al. (2007). Targeted inflammation during oncolytic virus therapy severely compromises tumor blood flow. Mol. Ther. *15*, 1686–1693.

Brun, J., McManus, D., Lefebvre, C., Hu, K., Falls, T., Atkins, H., Bell, J.C., McCart, J.A., Mahoney, D., and Stojdl, D.F. (2010). Identification of genetically modified Maraba virus as an oncolytic rhabdovirus. Mol. Ther. *18*, 1440–1449.

Cheung, H.H., Lynn Kelly, N., Liston, P., and Korneluk, R.G. (2006). Involvement of caspase-2 and caspase-9 in endoplasmic reticulum stress-induced apoptosis: a role for the IAPs. Exp. Cell Res. *312*, 2347–2357.

Chou, T.C., Motzer, R.J., Tong, Y., and Bosl, G.J. (1994). Computerized quantitation of synergism and antagonism of taxol, topotecan, and cisplatin against human teratocarcinoma cell growth: a rational approach to clinical protocol design. J. Natl. Cancer Inst. *86*, 1517–1524.

Chung, N., Zhang, X.D., Kreamer, A., Locco, L., Kuan, P.F., Bartz, S., Linsley, P.S., Ferrer, M., and Strulovici, B. (2008). Median absolute deviation to improve hit selection for genome-scale RNAi screens. J. Biomol. Screen. *13*, 149–158.

Glimcher, L.H. (2010). XBP1: the last two decades. Ann. Rheum. Dis. *69* (*Suppl 1*), i67–i71.

Hamilton, T.C., Young, R.C., McKoy, W.M., Grotzinger, K.R., Green, J.A., Chu, E.W., Whang-Peng, J., Rogan, A.M., Green, W.R., and Ozols, R.F. (1983). Characterization of a human ovarian carcinoma cell line (NIH:OVCAR-3) with androgen and estrogen receptors. Cancer Res. *43*, 5379–5389.

Hetz, C. (2009). The UPR as a survival factor of cancer cells: more than folding proteins? Leuk. Res. *33*, 880–882.

Kaufman, H.L., and Bines, S.D. (2010). OPTIM trial: a Phase III trial of an oncolytic herpes virus encoding GM-CSF for unresectable stage III or IV melanoma. Future Oncol. *6*, 941–949.

Lal, R., Harris, D., Postel-Vinay, S., and de Bono, J. (2009). Reovirus: rationale and clinical trial update. Curr. Opin. Mol. Ther. *11*, 532–539.

Liu, J., HuangFu, W.C., Kumar, K.G., Qian, J., Casey, J.P., Hamanaka, R.B., Grigoriadou, C., Aldabe, R., Diehl, J.A., and Fuchs, S.Y. (2009). Virus-induced unfolded protein response attenuates antiviral defenses via phosphorylation-dependent degradation of the type I interferon receptor. Cell Host Microbe *5*, 72–83.

Louie, K.G., Behrens, B.C., Kinsella, T.J., Hamilton, T.C., Grotzinger, K.R., McKoy, W.M., Winker, M.A., and Ozols, R.F. (1985). Radiation survival parameters of antineoplastic drug-sensitive and -resistant human ovarian cancer cell lines and their modification by buthionine sulfoximine. Cancer Res. *45*, 2110–2115.

Mannkind-Corporation. (2008). IRE-1alpha inhibitors. World Intellectual Property Organization WO *2008/154484*, A1.

Manzl, C., Krumschnabel, G., Bock, F., Sohm, B., Labi, V., Baumgartner, F., Logette, E., Tschopp, J., and Villunger, A. (2009). Caspase-2 activation in the absence of PIDDosome formation. J. Cell Biol. *185*, 291–303.

Moenner, M., Pluquet, O., Bouchecareilh, M., and Chevet, E. (2007). Integrated endoplasmic reticulum stress responses in cancer. Cancer Res. *67*, 10631–10634.

Müller, U., Steinhoff, U., Reis, L.F., Hemmi, S., Pavlovic, J., Zinkernagel, R.M., and Aguet, M. (1994). Functional role of type I and type II interferons in antiviral defense. Science *264*, 1918–1921.

Ottolino-Perry, K., Diallo, J.S., Lichty, B.D., Bell, J.C., and McCart, J.A. (2010). Intelligent design: combination therapy with oncolytic viruses. Mol. Ther. *18*, 251–263.

Parato, K.A., Lichty, B.D., and Bell, J.C. (2009). Diplomatic immunity: turning a foe into an ally. Curr. Opin. Mol. Ther. *11*, 13–21.

Sinkovics, J.G., and Horvath, J.C. (2008). Natural and genetically engineered viral agents for oncolysis and gene therapy of human cancers. Arch. Immunol. Ther. Exp. (Warsz.) *56* (*Suppl 1*), 3s–59s.

Stojdl, D.F., Abraham, N., Knowles, S., Marius, R., Brasey, A., Lichty, B.D., Brown, E.G., Sonenberg, N., and Bell, J.C. (2000a). The murine double-stranded RNA-dependent protein kinase PKR is required for resistance to vesicular stomatitis virus. J. Virol. *74*, 9580–9585.

Stojdl, D.F., Lichty, B., Knowles, S., Marius, R., Atkins, H., Sonenberg, N., and Bell, J.C. (2000b). Exploiting tumor-specific defects in the interferon pathway with a previously unknown oncolytic virus. Nat. Med. *6*, 821–825.

Stojdl, D.F., Lichty, B.D., tenOever, B.R., Paterson, J.M., Power, A.T., Knowles, S., Marius, R., Reynard, J., Poliquin, L., Atkins, H., et al. (2003). VSV strains with defects in their ability to shutdown innate immunity are potent systemic anti-cancer agents. Cancer Cell *4*, 263–275.

Tinel, A., and Tschopp, J. (2004). The PIDDosome, a protein complex implicated in activation of caspase-2 in response to genotoxic stress. Science *304*, 843–846.

Todd, D.J., Lee, A.H., and Glimcher, L.H. (2008). The endoplasmic reticulum stress response in immunity and autoimmunity. Nat. Rev. Immunol. *8*, 663–674.

Vähä-Koskela, M.J., Heikkilä, J.E., and Hinkkanen, A.E. (2007). Oncolytic viruses in cancer therapy. Cancer Lett. *254*, 178–216.

Vakifahmetoglu-Norberg, H., and Zhivotovsky, B. (2010). The unpredictable caspase-2: what can it do? Trends Cell Biol. *20*, 150–159.

Vembar, S.S., and Brodsky, J.L. (2008). One step at a time: endoplasmic reticulum-associated degradation. Nat. Rev. Mol. Cell Biol. *9*, 944–957.

Volkmann, K., Lucas, J.L., Vuga, D., Wang, X., Brumm, D., Stiles, C., Kriebel, D., Der-Sarkissian, A., Krishnan, K., Schweitzer, C., et al. (2011). Potent and selective inhibitors of the inositol-requiring enzyme 1 endoribonuclease. J. Biol. Chem. *286*, 12743–12755.

Wang, Q., Mora-Jensen, H., Weniger, M.A., Perez-Galan, P., Wolford, C., Hai, T., Ron, D., Chen, W., Trenkle, W., Wiestner, A., and Ye, Y. (2009). ERAD inhibitors integrate ER stress with an epigenetic mechanism to activate BH3-only protein NOXA in cancer cells. Proc. Natl. Acad. Sci. USA *106*, 2200–2205.